A STUDY OF WIRE CHAMBERS WITH HIGHLY SEGMENTED CATHODE PAD READOUT FOR HIGH MULTIPLICITY CHARGED PARTICLE DETECTION*

R. Debbe, J. Fischer, D. Lissauer, T. Ludlam, D. Makowiecki, E. O'Brien,
V. Radeka, S. Rescia, L. Rogers, G. C. Smith, D. Stephani, B. Yu
Brookhaven National Laboratory, Upton, New York 11973

S. V. Greene, T. K. Hemmick, J. T. Mitchell, B. Shivakumar
Yale University, New Haven, Connecticut 06511

Abstract

Investigations of interpolating cathode "pad" readout have been carried out for high multiplicity, two dimensional position sensitive detection of minimum ionizing particles and heavy ions. A detector configuration representing only 0.6% of a radiation length and covering an area of 26 cm by 16 cm, with over 1000 readout channels, has been developed. In a prototype chamber using this technique, a resolution of less than 100 μm (rms), for 5.4 keV x-ray, and differential non-linearity of $\pm 6\%$ have been achieved. The technique has also been demonstrated for detectors of much larger area.

I. Introduction

Experiments with high energy heavy ions at the BNL Alternating Gradient Synchrotron (AGS) and CERN Super Proton Synchrotron have shown the necessity of developing position sensitive detectors capable of resolving high multiplicity and high track density events as well as possessing a wide dynamic range to detect minimum ionizing particles and heavy ions. These requirements also apply to detectors for future Relativistic Heavy Ion Collider experiments. Such detectors will be essential at the Superconducting Super Collider, where large particle multiplicities and high counting rates will be encountered with a dynamic range only for minimum ionizing particles.

This paper describes the design, construction and testing of two types of position sensitive detectors. The "Pad Chamber" [1] is a detector with a cathode plane divided into a large number of rectangular pads (Figure 1). Anode wires are placed above the pads and field wires with slightly negative potential are placed between anode wires. All pads beneath one anode wire are interconnected by a resistive strip. Approximately every tenth pad is read out by a charge sensitive preamplifier. An avalanche created by a charged particle traversing the detector induces localized charge on several pads. The position of the avalanche can then be found by calculating the centroid of the charge collected from these pads [2]. Unambiguous pattern recognition is achieved because of this two dimensional segmented cathode layout. Monte Carlo studies have shown that a detector of this type, with 500 readout channels, 1000 electron rms noise, and a gas gain of 10^4, can resolve a minimum ionizing particle track multiplicity of 20 with an efficiency of 96% [3].

In general the rms resolution along the anode wire σ_x, is between 1% and 3% of l_a, where l_a is the spacing between readout nodes or amplifier connection points–see Figure 1. The ratio σ_x/l_a is limited by the equivalent noise charge to signal ratio ENC/Q_s.

The "Chevron Pad Detector", a wire chamber with chevron shaped pads as a cathode (Figure 2), has also been studied. The general operating characteristics of detectors with this type of cathode are described in a companion paper [4]. In the present work, we have built a small test chamber with interchangeable cathode planes to study quantitatively the linearity of various pad geometries, following some earlier simulations of this type of cathode [5]. Preliminary results of this work are reported in this paper.

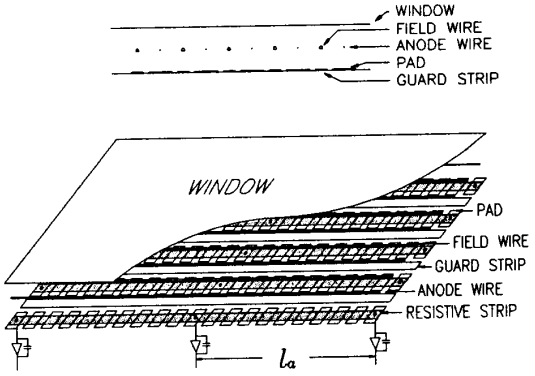

Fig. 1 Schematic of a pad chamber structure

*This research was supported in part by the U. S. Department of Energy: Contract DE-AC02-76CH00016

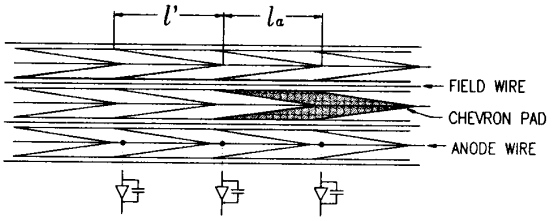

Fig. 2 A section of a chevron pad cathode

II. Chamber Design

A. Design and construction of the DC1 prototype

Monte Carlo simulations were used to choose the proper chamber geometry in order to achieve optimal performance. The results are reported in Refs. [1] and [3].

The cell structure of the prototype pad chamber (which we refer to as the DC1 prototype) is the following (Fig. 3): 25 gold plated tungsten wires of 17.5 μm diameter are placed 2 mm above the cathode pad plane; the anode wires spacing is 4 mm; 26 stainless steel wires of 125 μm are placed in between the anode wires. A cathode window made of 12.7 μm aluminized mylar is placed 2 mm above the wire plane. The anode wires are at a potential of about +1.2 kV. Field wires are normally at a slightly negative potential (less than 100 V) and the cathode window is grounded. The field wires maintain a uniform electric field around anode wires, so that avalanches occurring around the anode wires have the same gain. The field wires also define the cell boundaries and contribute to the reduction of dead regions between the cells.

The cathode pads as shown in Fig. 1 are 0.8 mm long in the anode wire direction (1 mm pitch) and 2 mm wide. We read out every tenth pad at 1 cm intervals. There are guard strips 1 mm wide placed between each pad row to reduce the charge shared between adjacent pad rows.

Because the detector is used as a tracking device in fixed target experiments where beam particles pass through the active area, it is necessary to have the ability to desensitize the beam area, therefore the center four anode wires are powered separately from the remainder.

The most challenging part of this project has been the manufacture of the cathode pad plane. There are two main constraints on this type of cathode plane. The material in the active area must be less than 1% of a radiation length to minimize multiple scattering in the experiment. In order to maintain uniform detection efficiency throughout the detector, and to achieve particle identification to some extent, we require the gain variation throughout the chamber be less than about $\pm$10%. This means the spacing between anode and cathode must be kept constant to within about $\pm$2%. The cathode plane was built using multilayer printed circuit board techniques(Fig. 3). The first step was to make a three layer board. The pads and guard strips were etched on the first layer. All the readout

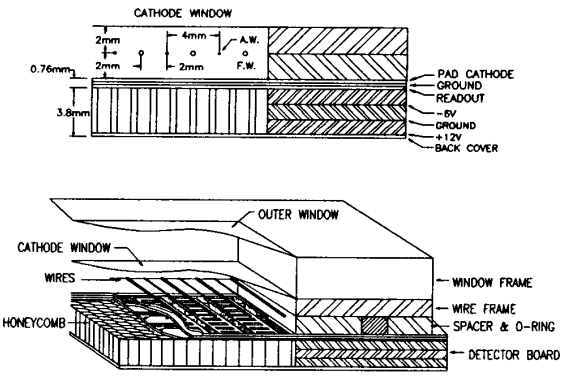

Fig. 3 The DC1 prototype structure.

leads were etched on the third layer and connected to the pads on the first layer by through plated holes. The second layer is a ground plane to shield the pads from the readout leads. It also helps to reduce the crosstalk between adjacent leads. The total thickness of this board is about 0.76 mm. The second step was to make a three layer board with the active area cut out. This board carries the power and ground needed by the preamplifiers. The thickness of this board is 3.8 mm. The next step was to fill the cut out area of the second board with a sheet of HEXCELL [6] polyimide honeycomb, and then glue together (under high pressure and temperature) these two boards plus a thin sheet of fiberglass. The honeycomb provides the structural rigidity necessary to maintain the required flatness of the cathode plane.

A layer of resistive polymer ink was applied over the pads on the finished cathode pad plane using a silk screening technique. We found that the resistive ink does not protect the copper pads from oxidizing, which would make the contact resistance to the pad unpredictable. In order to make good electrical contact with the resistive ink, the cathode pads were plated with a very thin layer of gold. The choice of resistive value between pads is such that the total resistance between readout nodes ,R_n, and the cathode pad capacitance per readout node, C_n, satisfies:

$$\tau_n = R_n C_n \approx \tau$$

where: τ_n is the RC time constance of one readout node.
τ is the zero to peak time of the shaping amplifier.

In our case, τ = 200 ns, C_n = 2.7 pF, we chose R_n = 80 kΩ, which means 8 kΩ between pads. The resistive ink requires a curing process at 210°C for 30 minutes. This temperature can be damaging to certain types of printed circuit board materials. We will discuss this further in the next section.

The preamplifier hybrid circuit cards (BNL IO-454-4) each contain three charge sensitive preamplifiers. In our AGS experiment, the outputs of the preamplifiers are fed to transformers through 2 meters of twisted pair ribbon cables and then through 50 meters of individually shielded

twisted pair cables, to shaping amplifiers with bipolar response.

There are two ways to calibrate the electronics chain. Since there is no calibration input on the preamplifier itself, we embedded a conductive strip over the readout leads connecting the pads and the preamplifier inputs. A pulser signal sent to the strip is capacitively coupled to the input of the preamplifier. We can also send a pulser signal to the anode wires, which induces a charge on the cathode pads under the wires, and read the output through the preamplifiers. In fact, the latter has been proven to be a very accurate calibration method, because it takes into account any differences in the preamplifier gain.

The rms noise in the electronics chain was measured by inducing a known amount of charge on the calibration strip and it was found to be equivalent to 1500 electrons (200 ns shaping time).

B. Design and construction of the DC1

The full sized pad chamber (DC1) is designed to be used in the AGS heavy ion experiment E814 as one of three tracking detectors. The cell structure is similar to that of the DC1 prototype, except that the anode wires to window spacing is 4 mm. The primary ionization therefore increases by 50% due to the increase of the gap. This allows the chamber to operate at a lower gas gain to maintain the same level of signal as in the DC1 prototype. Because of this asymmetrical cell geometry, however, a negative bias potential has to be applied to the window in order to obtain a near symmetrical field on both side of the anode wires. There are 40 anode wires and 41 field wires. The pads are 0.9 mm long and 2 mm wide. The pad pitch is 1.5 mm. The DC1 has an active area of 26 cm by 16 cm, with a total of 1016 readout channels. Since this detector is designed for use in a fixed target experiment, the track density varies across its active area. Different readout densities are used in the DC1 to match the track densities. In the central region where we expect maximum track density, the readout spacing is 6 mm (every 4th pad). In the outer region, readout separations of 12 mm (every 8th pad) and 15 mm (every 10th pad) are used.

The construction of the DC1 is different from the prototype. As mentioned earlier, the resistive ink is cured by baking the printed circuit board at a temperature of 210°C. But for a large detector such as the DC1, we found that it is extremely difficult to maintain the rigidity of the board under high temperature. On the other hand, the circuitry for over 1000 channels has to fan out to a much longer distance to match the preamplifier density. It is very difficult to make such a large board with very narrow traces without open or short circuits. So we chose another type of structure. Figure 4 shows a cross section of the DC1. Instead of making a single board, we made three boards. One is the cathode board, the other two are the preamplifier boards. The cathode board has three layers, which contain pads, ground and readout leads, respectively. Its thickness is 0.76 mm. We plated the pads with gold, applied resistive ink over the pads and cured the ink as required on this board. Then we glued a sheet of 6.35 mm thick fiberglass honeycomb on the back of the cathode board with epoxy and another sheet of fiberglass to the other side of the honeycomb. We found this technique to be straight forward and the flatness variation on the active area was measured to be within $\pm 40\mu m$. The readout leads from the active area are fanned out to the top and bottom side of the cathode board, and connected to rows of sockets. On the preamplifier boards, connectors were mounted at corresponding positions. The preamplifier boards are plugged into the cathode board. The readout leads on the preamplifier boards are further fanned out to the preamplifiers.

The total material of both detectors corresponds to about 0.6% of a radiation length.

The gas used in the detectors was 90% Ar and 10% CH_4, later switched to 50% Ar and 50% C_2H_6. The change of gas was to accommodate the requirement of the other drift chambers in the experiment.

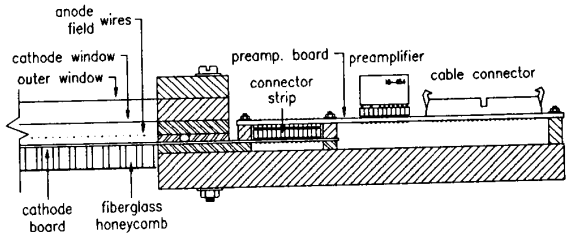

Fig. 4 A schematic cross section of the DC1.

III. Pad Chamber Performance

A. Position resolution versus anode charge

The position resolution from electronic noise alone for pad detectors with resistive charge division is determined as [7]:

$$FWHM \approx 3a_f \frac{l_a}{Q_s}\sqrt{\frac{\tau kT}{R_n}} = 3a_f \frac{l_a}{Q_s}\sqrt{\frac{\tau}{\tau_n}}\sqrt{kTC_n}$$

where: a_f is a constant factor ($2 \leq a_f \leq 3$).
Q_s is the amount of charge of the cathode signal.
T is the absolute temperature.
k is Boltzmann constant.

A shorter shaping time τ will improve the resolution. However, if $\tau < \tau_n$, the position linearity will degrade because the cathode signals are not completely collected by the readout electronics. The optimum choice is to make $\tau \approx \tau_n$. Under this condition, the position resolution given from the equation above is independent of the resistance between readout nodes[7].

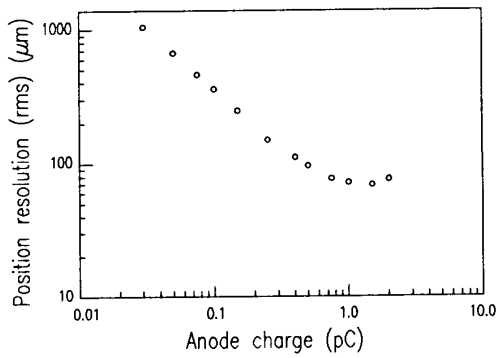

Fig. 5 Position resolution of the DC1 prototype as a function of anode charge. l_a = 1 cm. Anode charge was measured with a 200 ns shaping time. Gas was 90% Ar and 10% CH_4. 5.4 keV x-ray beam positioned in between readout nodes.

Absolute position resolution and linearity of the detectors has been measured by means of an electronic centroid finding system, in which the centroid of charge is determined by convolution of the sequentially switched outputs from several readout nodes with a linear centroid finding filter [7]. The test was performed with a 15 μm wide collimated x-ray beam and with a gas mixture of 90% Ar and 10% CH_4 . The anode charge was measured with a 200 ns shaping time. Figure 5 shows the behavior of the position resolution versus anode charge in the DC1 prototype with a readout node spacing of 1 cm. For Q_A up to approximately 0.2 pC, the resolution improves according to a $1/Q_A$ relationship, since the electronic noise is the only significant perturbing factor. For Q_A above 0.2 pC, however, the position resolution improves more slowly than $1/Q_A$ because of the influence of phenomena such as electron range and diffusion. A minimum value of about 70 μm (rms) was attained for $Q_A \approx 1.5$ pC. Higher charge levels cause progressive deterioration in resolution because of spreading of the avalanche along the anode wire.

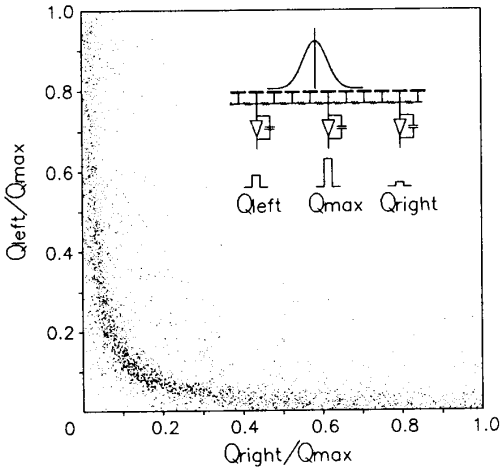

Fig. 6 Charge ratio plot from the DC1, with l_a=6mm, and a 50% Ar 50% C_2H_6 gas mixture. Radiation was 14 GeV protons.

Figure 6 shows one of the characteristics of this type of detector. By choosing signals from three adjacent readout nodes such that the one in the middle has maximum signal Q_{max}, and plotting the ratio of the signal from the node on the left Q_{left} to Q_{max}, versus the ratio of Q_{right} to Q_{max}, one produces this charge ratio plot [8]. By measuring the width of this hyperbolically shaped band, one can determine the noise to signal ratio, and therefore the position resolution. The data for Figure 6 were taken from the DC1 during a proton beam test at the AGS with a Fastbus ADC system. The anode charge level was approximately 0.15 pC. The resolution estimated from the width of the band is about 120 μm (rms) (l_a= 6 mm).

B. Position linearity of the detector

A convenient measure of position non-linearity is the differential non-linearity, which can be obtained from a position spectrum for uniform irradiation. Measurements have been made by obtaining a uniform irradiation response (UIR), with 5.4 keV x-rays, from a section of the anode wire. The preamplifier signals were fed to the centroid finding system and the resulting position signals analyzed with a pulse height analyzer. Figure 7(a) shows the UIR across eight readout nodes of the DC1 prototype. The positions of the readout nodes, separated by 1 cm, correspond to the tick marks on the abscissa. Differential non-linearity is better than ±6%. Figure 7b shows the absolute position error derived by evaluating integral non-linearity. The reconstructed position can be derived from this equation:

$$y(x) = a + \frac{1}{b-a}\int_{-\infty}^{+\infty} N(y)dy \int_{-\infty}^{x} \frac{1}{N(y)}dy$$

where: x is the true position, assuming the irradiation is uniform and is limited to $a \leq x \leq b$.
y is the reconstructed position.
$N(y)$ is the counts from the UIR spectrum on a pulse height analyzer.

If the differential non-linearity is small, one can consider the UIR spectrum as function of the true position u instead of reconstructed position y. This results in the following approximation:

$$y(x) \approx a + \frac{1}{b-a}\int_{a}^{b} N(u)du \int_{a}^{x} \frac{1}{N(u)}du$$

The position error in Figure 7(b) was found to be less than ±60μm.

C. Position resolution as a function of position

Position resolution as a function of position has been quantitatively discussed in Reference [7]. However, one can get a qualitative understanding by using a simple model.

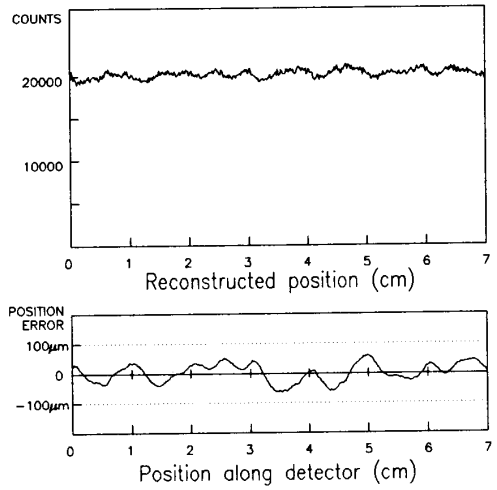

Fig. 7(a) X-ray UIR spectrum of a section of the DC1 prototype shows the differential non-linearity.
(b) Absolute position error derived from the spectrum above. The tick marks on the abscissa correspond to the readout nodes. Gas was 90% Ar and 10% CH_4. Time constant was 1.4 μs.

Assume that the centroid finding was obtained from three readout nodes (which is true for most cases), node B which has the maximum signal is at the origin and the readout node spacing is set to unity. We have:

$$x = \frac{Q_c - Q_a}{Q_a + Q_b + Q_c}.$$

We set:

$$Q_s = Q_a + Q_b + Q_c$$

then:

$$\begin{aligned} \delta x &\approx \frac{1}{Q_s}(\delta Q_c - \delta Q_a - x(\delta Q_a + \delta Q_b + \delta Q_c)) \\ &= \frac{1}{Q_s}(-\delta Q_a(1+x) - \delta Q_b x + \delta Q_c(1-x)). \end{aligned}$$

Assuming the noise from all three nodes is equal in amplitude and not correlated, i.e.

$$\delta Q_a = \delta Q_b = \delta Q_c = \delta Q$$

then:

$$\begin{aligned} \delta x &\approx \frac{1}{Q_s}\sqrt{(\delta Q_a(1+x))^2 + (\delta Q_b x)^2 + (\delta Q_c(1-x))^2} \\ &= \frac{\delta Q}{Q_s}\sqrt{2+3x^2}. \end{aligned}$$

The possible range of x is $(-0.5 \leq x \leq +0.5)$ (otherwise node B will not be the center of the three nodes for centroid finding). The position resolution δx is proportional to the noise to signal ratio, $\delta Q/Q_s$, and has a minimum value when $x = 0$ (right on a readout node) and has a maximum value when $x = 0.5$ (in the middle of two nodes). Our measurements have confirmed this relationship.

D. Position resolution and resistance uniformity

For detectors with this type of resistive charge division, it is obvious that the position linearity is mainly determined by the uniformity of the resistance values of individual resistors between pads. Figure 8 shows a UIR spectrum from a section of the DC1 where the worst resistance non-uniformity was found. Notice one of the resistors has a resistance value 70% larger than the average. The position error caused by this resistor is about 500 μm. A computer simulated spectrum which is simply based on the resistive values shows good resemblance to the spectrum obtained by uniformly irradiating the detector. In principle one can use the simulated results to correct the reconstructed positions if one can measure every single resistor on the detector (in our case, 5 to 7 thousand of them). Clearly, a better way of improving linearity is to control the resistance values within a tolerable range. Our study based on computer simulation shows that a $\pm 10\%$ variation in resistance values will result in a $\pm 100\mu$m position error (with $l_a = 6$ mm). The precision of silk screening resistors is no better than $\pm 10\%$. The possibility of trimming the resistors has been investigated. One of the printed circuit boards for the DC1 prototype was abrasively trimmed by a commercial facility. The non-uniformity was $\pm 5\%$. This can be translated into a $\pm 5\%$ differential non-linearity across the whole detector. The position error is more sensitive to local changes (within readout node spacing) in resistance value rather than global changes.

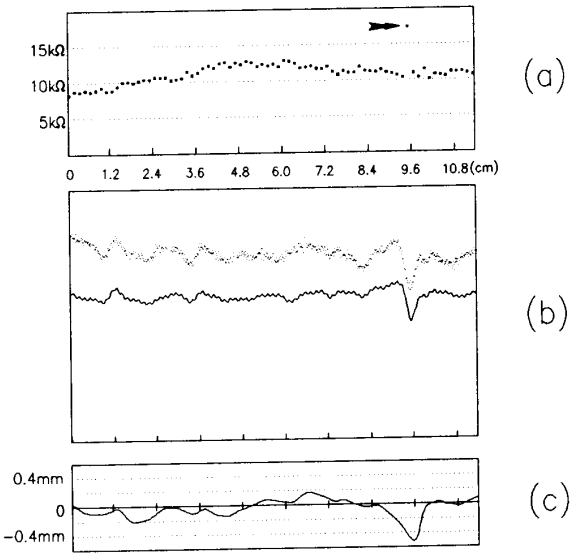

Fig. 8 Effect of non-uniformity of resistors in a pad chamber.
(a) Values of the resistors in a section of the DC1. The tick marks on the abscissa correspond to the readout node positions;
(b) The spectrum on top is the result from a uniform x-ray irradiation over this section of detector. The spectrum on the bottom is the result from a computer simulation.
(c) Absolute position error obtained from computer simulation.

IV. Chevron Pad Chamber

Two detectors with chevron cathode planes have been built and used as tracking devices along with the DC1 in the E814[4]. We have also built a small chamber with interchangeable chevron cathode planes to study the linearity and resolution of this type of cathode. The test chamber has five anode wires, with diameter 18 μm, three of which are connected to a preamplifier. 125 μm stainless steel wires are placed in between anode wires as the field wires. Cell structure is the same as in the DC1. However, the frame that holds the cathode window can be mounted either facing up, or facing down. This gives the window to wires spacing a value of either 4 mm (as in the DC1) or 2 mm (as in the DC1 prototype).

Figure 2 shows a section of a chevron cathode plane we studied. All the pads are read out by charge sensitive preamplifiers. In this scheme, position sensing is achieved by geometrical charge division. There are many parameters one can change, such as length, width, gap width and shape, to improve the chamber linearity. Each cathode plane tested has three rows of chevron pads with the same l_a, but different l' (defined in Fig.2) i.e. $l' = l_a$, $l' = 1.05l_a$ and $l' = 1.1l_a$.

The testing of the chevron pad chamber was performed with the same centroid finding system as described earlier and 5.4 keV x-rays. A total of five different cathode planes were tested. Each cathode plane tested has three rows of chevron pads with slight differences. The first row has $l' = 1.1l_a$, the second row has $l' = 1.05l_a$, and the third row has $l' = l_a$. Figure 9 shows the UIR spectra obtained from one of the cathodes. Spectra from other cathodes also suggest that making l' slightly longer than l_a will improve the linearity of the chevron pad chamber. Similar behavior has been observed with zigzag strip cathodes [10].

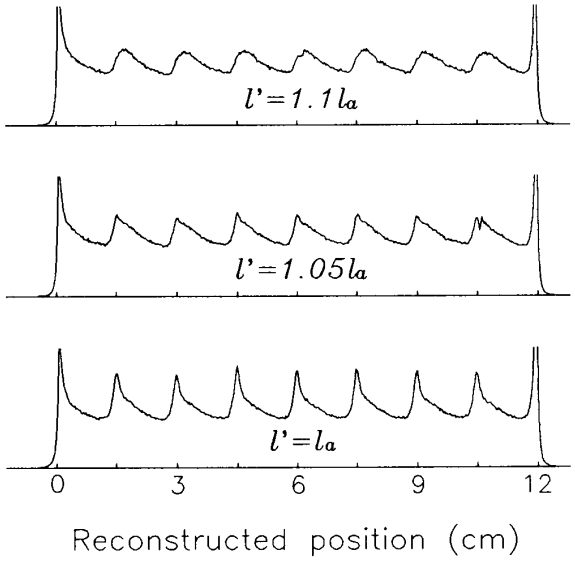

Fig. 9 Three UIR spectra from chevron chamber with different l'/l_a ratios. l_a = 1.5 cm.

One interesting phenomenon we observed is the effect of the anode avalanche angular localization on the position accuracy and linearity of the chamber [9]. If a narrow beam of x-rays is incident on the detector from directly above one of the anode wires, x-rays are absorbed both above and below this wire. The induced charge on the chevron cathode pads for events initiating an avalanche on top of the wire is different in time development and charge distribution from that for events from below the wire. This can result in a considerable difference in the reconstructed centroid position. Figure 10 shows the reconstructed position spectra under three different conditions. Figure 10(a) was the result when the anode wires were 2 mm from both the cathode plane and the cathode window. The test was to measure the resolution of the chamber at different positions. The x-ray beam was moved in 1 mm steps from one readout node to the next. However, the reconstructed position spectrum started to split into two distinct peaks as the x-rays moved away from a readout node. The maximum separation is 0.25 mm, 4% of the readout node spacing. Figure 10(b) shows the result with the anode wires 2 mm away from the cathode pad plane and 4 mm away from the window. As one can see, the "window side" events are almost twice as many as the "pad side" events. A special filtering technique [9] allows us to select one type of events over the other. The resulting curves for both "window side" events (solid line) and "pad side" events (dotted line) are clean narrow peaks as shown in Figure 10(c).

This splitting of centroid position for x-ray events is more pronounced with a long sampling time constant (the time constant in our centroid finding system is about 1.4 μs) and a small anode-cathode spacing. For the case of a finely collimated beam of charged particles, a single position peak will be observed. Fluctuation of ionization clusters along the particle tracks will, however, cause a

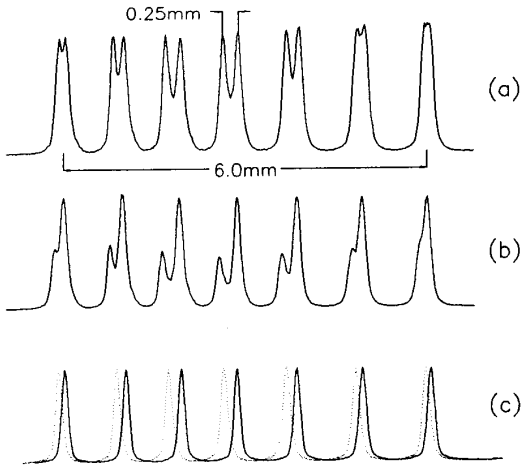

Fig. 10 Reconstructed position spectra of chevron chamber under different conditions. l_a = 6 mm.
(a) Symmetrical cell structure, no event filtering.
(b) Asymmetrical cell structure, no event filtering.
(c) Asymmetrical cell structure, with event filtering.

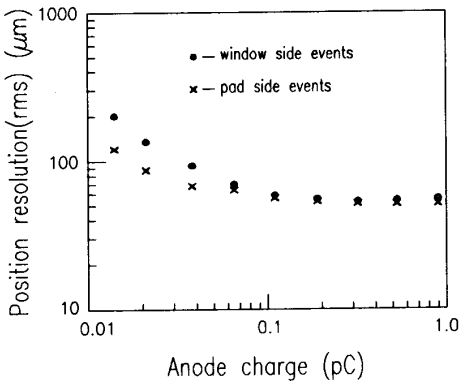

Fig. 11 Position resolution of a chevron chamber as a function of anode charge. l_a = 6mm, The anode charge was measured with a 200 ns shaping time. Gas was 50% Ar and 50% C_2H_6 mixture.

broadening of the position peak. A shorter time constant (such that the positive ions drifting in opposite directions have not moved far away from the anode wire) or a larger anode-cathode spacing (such that the displacement of the ions is relatively small) will reduce the splitting and the broadening.

The position resolution of the chevron detector we tested is very good, largely because of the lack of resistors as a noise source. For a cathode plane with 6 mm readout node spacing, using the filter technique, we can easily achieve a resolution better than 60 μm (rms) at a moderate charge level. Figure 11 shows the resolution as a function of anode charge.

V. Discussion

Both types of pad detector have been built and used in the E814 heavy ion experiment at the AGS. Their ability to handle high particle multiplicity and provide unambiguous two-dimensional position information (1 - 3% readout node spacing along the wire direction) affords a very powerful detector technique. Pad chambers with resistive charge division such as the DC1 prototype and the DC1 can provide excellent position resolution and linearity. By using laser or abrasive trimming of resistors, one can expect to reduce the differential non-linearity down to the 2% level. Resistor trimming on a detector of larger active area becomes more difficult. Therefore this detector technique will be most conveniently used on detectors with relatively small active areas, or where large cathodes can be subdivided into modules. Detectors of similar type with discrete resistors mounted on the back of cathode planes have been studied at CERN [11]. On the other hand, chevron pad detectors, with geometrical charge division, are most suited for larger active areas with relaxed position linearity and resolution requirement. We have built a detector 2 m by 0.5 m in size, using a chevron cathode as one of the planes [4]. The linearity of the chevron cathode can be improved by choosing the optimum geometry. We are now investigating finer chevrons which, based on computer simulation [12], show dramatic reduction in non-linearity. Fabricating a cathode for such chevron shapes and good linearity will be more difficult. On the other hand, the non-linearity of the chevron for a given shape has a very regular periodicity. In principle, by measuring the response of one pad, one can use it to set up a correction for all of the pads of the same shape with a very high accuracy.

Acknowledgements

Detectors of this nature involve many areas of technology and requires the assistance of many individuals. In particular we would like to acknowledge the useful discussions with C. Woody and help from T. Willis during the testing of the detectors. The production of various printed circuit boards was carefully done by A. De Libero, R. Angona and P. Borello. A large portion of the detectors were constructed by R. Chanda. E. Von Achen helped throughout the detector assembly.

References

[1] R. Debbe *et al.*, "MWPC with highly segmented cathode pad readout," *Nucl. Instrum. and Methods* vol. A283, pp. 772-777 (1989).

[2] J. L. Alberi and V. Radeka, "Position sensing by charge division," *IEEE Trans. Nucl. Sci.* NS-23, pp. 251-258 (1976).

[3] T. Ludlam, R. Debbe, and V. Radeka, "Many-track chamber: A design for T1," BNL E802 note (Oct. 1985).

[4] J. Fischer *et al.*, "A many-particle tracking detector with drift planes and segmented cathode readout," These proceedings.

[5] R. Chase, "Evaluation of the linearity of position measurement with chevron-shaped cathodes by scale-up simulation," BNL Internal note (Summer 1987).

[6] Trade mark of HEXELL Corp., 11711 Dublin Blvd., Dublin, CA 94568.

[7] V. Radeka and R. Boie, "Centroid finding method for position-sensitive detectors," *Nucl. Instrum. and Methods* vol. 178, pp. 543-554 (1980).

[8] J. Chiba *et al.*, "Study of position resolution for cathode readout MWPC with measurement of induced charge distribution," *Nucl. Instrum. and Methods* vol. 206, pp. 451-463 (1983).

[9] G. Smith, J. Fischer, and V. Radeka, "Photoelectron range limitations to the spatial resolution for x-rays in gas proportional chambers," *IEEE Trans. Nucl. Sci.* NS-31, pp. 111-114 (1984).

[10] E. Mathieson and G.C.Smith, "Reduction in non-linearity in Position-Sensitive MWPCs," *IEEE Trans. Nucl. Sci.* NS-36,pp 305-310 (1989).

[11] H. Beker *et al.*, "Test results with a novel high-resolution wire chamber with interpolative pad readout," *Nucl. Instrum. and Methods* vol. A283, pp. 762-766 (1989).

[12] E.Mathieson, private communication, 1989.